International Journal of Pharmaceutics 434 (2012) 391–398

Contents lists available at SciVerse ScienceDirect

International Journal of Pharmaceutics

journal homepage: www.elsevier.com/locate/ijpharm

Pharmaceutical Nanotechnology

Interaction of miltefosine with intercellular membranes of stratum corneum and biomimetic lipid vesicles

Lais Alonso[a], Sebastião Antônio Mendanha[a], Cássia Alessandra Marquezin[a], Marina Berardi[b], Amando Siuiti Ito[b], A. Ulises Acuña[c], Antonio Alonso[a,*]

[a] Instituto de Física, Universidade Federal de Goiás, Goiânia, GO, Brazil
[b] Faculdade de Filosofia Ciências e Letras de Ribeirão Preto, Universidade de São Paulo, Ribeirão Preto, SP, Brazil
[c] Instituto de Química Física "Rocasolano", C.S.I.C., Serrano 119, E-28006 Madrid, Spain

ARTICLE INFO

Article history:
Received 23 December 2011
Received in revised form 17 May 2012
Accepted 3 June 2012
Available online 9 June 2012

Keywords:
EPR
Fluorescence
Spin label
Miltefosine
Stratum corneum
Phospholipid bilayer

ABSTRACT

Miltefosine (MT) is an alkylphospholipid approved for breast cancer metastasis and visceral leishmaniasis treatments, although the respective action mechanisms at the molecular level remain poorly understood. In this work, the interaction of miltefosine with the lipid component of stratum corneum (SC), the uppermost skin layer, was studied by electron paramagnetic resonance (EPR) spectroscopy of several fatty acid spin-labels. In addition, the effect of miltefosine on (i) spherical lipid vesicles of 1,2-dipalmitoyl-*sn*-glycero-3-phosphatidylcholine (DPPC) and (ii) lipids extracted from SC was also investigated, by EPR and time-resolved polarized fluorescence methods. In SC of neonatal Wistar rats, 4% (w/w) miltefosine give rise to a large increase of the fluidity of the intercellular membranes, in the temperature range from 6 to about 50 °C. This effect becomes negligible at temperatures higher that ca. 60 °C. In large unilamelar vesicles of DPPC no significant changes could be observed with a miltefosine concentration 25% molar, in close analogy with the behavior of biomimetic vesicles prepared with bovine brain ceramide, behenic acid and cholesterol. In these last samples, a 25 mol% molar concentration of miltefosine produced only a modest decrease in the bilayer fluidity. Although miltefosine is not a feasible skin permeation enhancer due to its toxicity, the information provided in this work could be of utility in the development of a MT topical treatment of cutaneous leishmaniasis.

Published by Elsevier B.V.

1. Introduction

Human leishmaniasis is caused by different species of protozoa parasites of the *Leishmania* genus. This tropical disease is endemic in many countries, and the most severe visceral infection is fatal if untreated. The treatment of the disease relies on chemotherapy (Alvar et al., 2006), with organic pentavalent antimonials administered parenterally in high doses requiring patient hospitalization. An alternative therapy is based on amphotericin B deoxycholate (AmB), an antifungal antibiotic that can be nephrotoxic and should be administered with close patient monitoring (Croft et al., 2006). Alkylphosphocholines (APCs) represent a class of antitumor agents that have been shown to induce apoptosis in tumor cells, but their exact mode of action is only partially known. Miltefosine (hexadecylphosphocholine, MT) is a synthetic alkylphosphocholine originally developed for its antineoplastic properties, but also presenting a potent leishmanicidal activity (Kuhlencord et al., 1992; Croft et al., 2005). In recent years, MT afforded the first successful oral therapy of human visceral leishmaniasis in field-trials, with mild secondary effects (Sindermann and Engel, 2006; Soto and Soto, 2006), and is currently licensed for the treatment of visceral and cutaneous leishmaniasis in India, Colombia and Germany.

Despite the relatively large advances on the clinical applicability of MT it is noticeable the incomplete information on the drug's primary targets, *in vivo* metabolic processes and pharmacokinetics (Croft et al., 2003; Saugar et al., 2007; Barrat et al., 2009). Even considering that MT in the peroral form is effective for treatment of visceral leishmaniasis (Berman, 2006), its use as a chemotherapeutic agent upon peroral or intravenous administration may be limited by the harmful effect on epithelial cells of the GI tract (Jha et al., 1999) and on erythrocytes that leads to hemolysis (Wieder et al., 1999). In this context, knowledge about the interaction of the drug, a membrane-active compound, with the uppermost skin layer, the stratum corneum (SC), becomes particularly relevant.

The permeability barrier of the skin is located in the uppermost epidermal layer, the SC, composed of corneocytes surrounded by

Abbreviations: MT, miltefosine; 5-DMS, methyl 5-doxyl-stearate; 16-DMS, methyl 16-doxyl-stearate; 5-DSA, 5-doxyl stearic acid; Ahba, 2-amino-N-hexadcyl benzamide; SC, stratum corneum; DPPC, 1,2-dipalmitoyl-*sn*-glycero-3-phosphatidylcholine.

* Corresponding author. Tel.: +55 62 3521 1470; fax: +55 62 3521 1014.
E-mail address: alonso@if.ufg.br (A. Alonso).

0378-5173/$ – see front matter. Published by Elsevier B.V.
http://dx.doi.org/10.1016/j.ijpharm.2012.06.006

a multilamellar lipid matrix. Anucleate corneocytes are keratin-filled dead cells containing a peripheral cornified envelope of cross-linked proteins surrounded by a covalently bound lipid envelope composed mainly of ω-hydroxyceramides (Wertz and Downing, 1987). The intercellular region contains a lipid mixture, consisting basically of ceramides, free fatty acids and cholesterol that are ordered in multilayered structures known as lipid lamellae. The lipid envelope forms a layer that may function as a template or scaffold for the organization of the intercellular lipids (Hohl, 1990). The lipid composition of SC is unusual and very complex containing twelve types of ceramides, formed by long-chains fatty acid moieties (nonhydroxy, α-hydroxy, or ester-linked ω-hydroxy) amide-linked to sphingoid moieties (sphingosine, dihydro-sphingosine, phytosphingosine, or 6-hydroxy-sphingosine) (Masukawa et al., 2008). The fraction of chemically bound hydroxyceramide is about 1.4% of tissue dry weight for man (Wertz et al., 1989) and 2.1 for pig SC (Wertz and Downing, 1987), whereas the fraction of unbound lipids in pig SC that can be removed by exhaustive extraction with chloroform:methanol mixtures corresponds to about 14% (Swartzendruber et al., 1987).

Electron paramagnetic resonance (EPR) spectroscopy of fatty-acid spin probes has been used before to obtain information about SC membranes in the intact tissue (Alonso et al., 1995, 1996, 2000; de Queirós et al., 2005). It is well documented that the permeability of the SC to water and other substances increases with SC hydration; similarly, it has been shown by EPR of spin-labeled fatty-acid probes that the increase in tissue hydration leads to an increase in membrane fluidity (Alonso et al., 1995, 1996). Important information was obtained by comparing lipid chain dynamics in vesicles prepared with lipids extracted from SC with the dynamics in intact tissue. These results indicated a completely different lipid dynamics in the two types of samples, suggesting that the lipids covalently attached to proteins restrict the rotational diffusion of intercellular lipids, and that this is a fundamental property associated to the physical barrier function of SC (Alonso et al., 2000). More recently, EPR spectroscopy was used to show that the treatment of SC with skin permeation enhancers of monoterpene class, such as menthol, cineole and limonene, leads to increased lipid fluidity (dos Anjos et al., 2007a,b) and increased partition coefficient of small water-soluble spin probes TEMPO (dos Anjos and Alonso, 2008) and DTBN (Camargos et al., 2010) into SC membranes.

In this work, the effect of miltefosine on SC membranes was investigated by EPR and fluorescence spectroscopy techniques, and interpreted in terms of changes in membrane fluidity. In the present context, "fluidity" is used to estimate changes in the extent of order (a static property) and dynamics of membrane lipids, as discussed below. It was observed from the EPR spectra of spin probes that the presence of MT causes a large increase in the membrane fluidity of SC. However, the effect of the drug on spherical vesicles prepared from bovine brain ceramide, behenic acid and cholesterol was only a small reduction in fluidity. On the other hand, no change was observed on DPPC large unilamellar vesicles (LUV's) until a MT concentration of 25 mol%. The LUV's results are similar to those obtained by fluorescence techniques, using 2-amino-N-hexadcyl benzamide (Ahba) as a lipophilic probe to monitor the MT interaction with DPPC lipid bilayers.

2. Materials and methods

2.1. Chemicals

The phospholipid 1,2-dipalmitoyl-*sn*-glycero-3-phosphocholine (DPPC) was purchased from Avanti (Avanti Polar Lipids, Inc., Alabaster, AL); miltefosine (Fig. 1), ceramide from bovine brain, behenic acid, cholesterol and the spin labels methyl 5- and 16-doxyl-stearate (5- and 16-DMS) and 5-doxyl stearic acid (5-DSA) were purchased from Sigma (Chem. Co., St. Louis, MO). The lipophilic probe 2-amino-N-hexadcyl benzamide (Ahba) was prepared as previously described (Marquezin et al., 2006). All other chemicals were of the highest grade available.

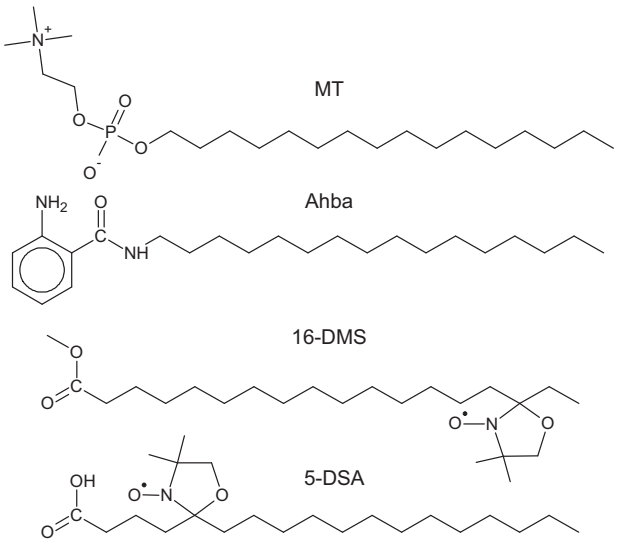

Fig. 1. Chemical structure of two spin labels (16-DMS and 5-DSA), miltefosine (MT) and the fluorescent probe Ahba.

2.2. Preparation of unilamellar spherical lipid vesicles

5 mg of a mixture of phospholipid and spin probe, at a lipid:probe molar ratio of 150:1, were dissolved in 1 mL of chloroform and dried under a nitrogen stream. Samples containing also 25 mol% MT were prepared by dissolving the three components in the organic phase at appropriate proportions. The residual solvent was removed by overnight vacuum-drying. In the hydration step, the dry samples were incubated in PBS (5 mM phosphate, 150 mM NaCl and 0.2 mM EDTA, pH 7.4) for 5 min at 60 °C and vortexed several times. To produce unilamellar vesicles, the sample volume was adjusted to 0.7 mL with PBS buffer and extruded through 0.1 μm-pore polycarbonate filters using a mini-extruder (Avanti Polar Lipids, Inc., Alabaster, AL). The extrusion process, consisting of about 21 serial passes, was performed at 55 °C. The volume of water in the sample was reduced by flowing nitrogen gas to obtain a lipid concentration of about 50 mM. Finally, the vesicle suspension was transferred to a capillary and flame-sealed.

2.3. Preparation of SC membranes

SC membranes of neonatal Wistar rats less than 24 h old were prepared as described elsewhere (Alonso et al., 1995, 1996, 2001; de Queirós et al., 2005; Camargos et al., 2010). Briefly, after the animal was killed, its skin was excised and placed in a beaker containing distilled water. In order to separate the SC from the epidermis, the skin was placed for 5 min in a desiccator containing ammonium hydroxide (only water vapor saturated with ammonium hydroxide is in contact with the SC). Then, the skin was left floating on distilled water with SC facing the air and, after 2 h, the outer skin was placed in contact with filter paper and the SC was carefully separated from the remaining epidermis by friction. Subsequently, the SC was transferred to a Teflon-coated screen, washed with distilled water and allowed to dry at room temperature. The

membranes were stored in a desiccator containing silica gel, under a moderate vacuum.

In an alternative technique, the SC is separated from the epidermis by heat treatment. However, we noticed that in the case of EPR experiments this method gives rise to an additional high-mobility component in the spectrum of the 5-DSA probe, although the main features of the spectra are identical using both techniques. Since this may be due to residual contamination of SC from epidermal lipids we preferred the ammonium hydroxide protocol described above.

2.4. Spin labeling and miltefosine treatment of SC

A piece of dry SC about 3 mg was weighed and then hydrated by incubating 20 min at room temperature in 50 μL of acetate-buffered saline (10 mM sodium acetate, 150 mM NaCl and 1 mM EDTA, pH 5.5). The pH of SC *in vivo* is approximately 5.5 (Öhman and Vahlquist, 1998). A small aliquot (1 μL) of a stock solution of spin label in ethanol (10 mM) was spread on a glass plate and, after the solvent evaporated, the SC membrane fragment was suspended with about 50 μL of buffer on the same site where the spin label was placed and gently mixed with a small stick for about 10 min. After spin labeling, the SC membranes were treated with MT using the same procedure described above. An appropriated aliquot of ethanol solution containing MT (15 mg/mL) was applied on a glass plate. After the ethanol evaporation, the SC membrane with a small aliquot of buffer was put on the MT film. The SC was gently mixed for about 15 min and then introduced into 1-mm I.D. capillary for EPR measurements. The excess solvent was removed and the capillary flame sealed.

2.5. EPR spectroscopy

EPR spectra were acquired with a Bruker ESP 300 spectrometer (Bruker, Rheinstetten, Germany) equipped with an ER 4102 ST resonator and a temperature controller. The instrument settings were: microwave power, 2 mW; modulation frequency, 100 kHz; modulation amplitude, 1.0 G; magnetic field scan, 100 G; sweep time, 168 s; and a detector time constant of 41 ms. The sealed capillary containing the sample was introduced into a 3-mm I.D. quartz tube containing mineral oil and a fine-wire thermocouple to monitor the sample temperature. EPR spectra simulations were performed using the NLLS program developed by Freed and coworkers (Budil et al., 1996). This program allows a single spectrum to be fitted with a model of two spectral components having different mobility and magnetic tensor parameters, providing the relative population and the associated rotational diffusion rates. In the spectral calculations, the NLLS program includes the magnetic *g*- and *A*-tensors and the rotational diffusion tensor, *R*, which are expressed in a system of Cartesian axes fixed in the spin-labeled molecule. To reduce the number of fitting parameters, the average rotational diffusion rate, R_{bar}, was calculated using the relation $R_{bar} = (R_{per}^2 \cdot R_{par})^{1/3}$, where R_{per} is the perpendicular and R_{par} is the parallel component of the rotational diffusion tensor (Budil et al., 1996). In this work, the spectra were simulated with a model of one or two spectral components (the component of higher stiffness and polarity was denoted as component 1 and the other as component 2). Similar to previous studies (Alonso et al., 2001, 2003), the magnetic parameters were determined based on a global analysis of the overall spectra obtained in this work, and all of the EPR spectra were simulated using the same predetermined parameters. Input parameters of tensors *g* and *A* for the two-spectral components, here denoted components 1 and 2, were: $g_{xx}(1) = 2.0083$; $g_{xx}(2) = 2.0087$; $g_{yy}(1) = 2.0060$; $g_{yy}(2) = 2.0062$; $g_{zz}(1) = 2.0022$; $g_{zz}(1) = 2.0026$; $A_{xx}(1) = 6.0$; $A_{xx}(2) = 5.5$ G; $A_{yy}(1) = 6.0$ G; $A_{yy}(2) = 5.5$ G; $A_{zz}(1) = 33.0$ G and $A_{zz}(2) = 32.1$ G.

In the fast motion regime, EPR spectra were simulated using the EPRSIM (version 4.99) software program (Arsov et al., 2002; Stopar et al., 2006). The input parameters for the magnetic interaction tensors *A* and *g* were the same for NLLS mentioned above. These parameters were corrected linearly by the fitting program through polarity correction factors applied on the trace of the *A*- and *g*-tensors, denoted by parameters p_A and p_g, respectively. While NLLS generates the average rotational diffusion rate R_{bar}, the EPRSIM provides τ_c, the rotational correlation time, $\tau_c = (1/6)R_{bar}$.

2.6. Optical absorption and fluorescence measurements

Optical absorption spectra were registered on a Amersham Ultrospec 2100 pro spectrophotometer. A Hitachi F-7000 spectrofluorimeter, with polarizer filters for anisotropy experiments, was used for steady state fluorescence measurements. Time-resolved fluorescence intensity and anisotropy experiments were made in an apparatus based on the time-correlated single photon counting method. The excitation source was a Tsunami 3950 Spectra Physics titanium–sapphire laser, pumped by a Millenia X Spectra Physics solid-state laser. The pulse repetition rate was 8.0 MHz and the laser wavelength 310 nm, extracted from a third harmonic generator; these excitation pulses were directed to an Edinburgh FL900 spectrometer. The fluorescence photons were detected by a refrigerated Hamamatsu R3809U microchannel plate photomultiplier. A Soleil–Babinet compensator in the excitation beam and a Glann–Thomson polarizer in the emission beam were used in anisotropy experiments. The instrument response function was typically 100 ps FWHM, with a time resolution of 12 ps/channel. The experimental decay curves were fitted to multi-exponential functions, and the quality of the fit was determined by the analysis of the reduced-χ^2 and by inspection of the residuals distribution.

3. Results

3.1. Effect of miltefosine on DPPC bilayers

The fluidity of unilamellar vesicles of DPPC labeled with several spin probes with and without 25 mol% of MT showed no significant differences, both below and above the temperature of the main thermal phase transition of the bilayer (42 °C). For a better appreciation of the similarity between pure DPPC and DPPC with MT, the EPR spectra are shown overlayed in Fig. 2 for several spin labels and temperatures. In the case of spin label 5-DSA (Fig. 2, left column), a sample of DPPC containing up to 35 mol% MT was also measured but no change in the spectra could be detected.

The interaction of MT with the lipid bilayer of DPPC vesicles was also studied by fluorescence methods using the fluorescent probe Ahba. It has been previously shown that this probe probe inserts into DPPC lipid bilayers and aligns parallel to the long chains of the lipid molecules in the vesicles (Marquezin et al., 2006), fluorescing at 404 nm under excitation at 330 nm. Here we observed that the addition of MT did not modify substantially the probe absorption and emission wavelength, giving rise only to a 10% increase in the fluorescence intensity. A single-exponential fluorescence lifetime was determined from the experimental decay curves, with a modest increase from 8.34 ns to 8.49 ns with the addition of MT (Fig. 3). The steady-state fluorescence anisotropy value of Ahba in pure DPPC vesicles, 0.034 at 25 °C, was comparable to that previously measured in the same conditions (Marquezin et al., 2006), and the addition of MT did not change significantly these values. The experimental decay of the fluorescence anisotropy of Ahba in DPPC

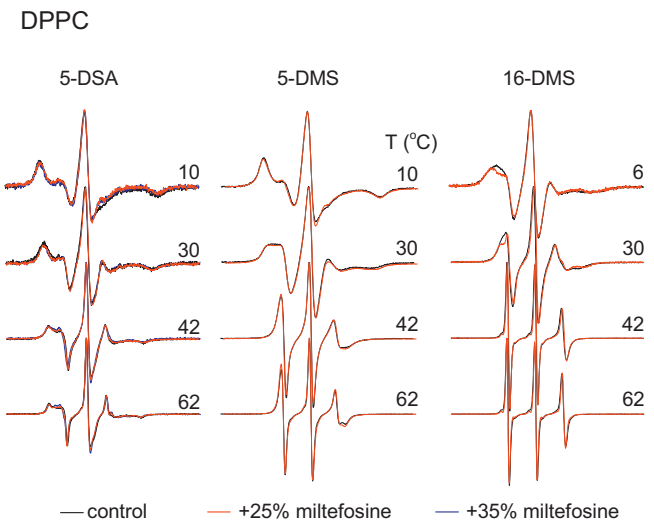

Fig. 2. The effect of miltefosine (MT) on the EPR spectra of 5-DSA, 5-DMS and 16-DMS spin labels incorporated to large unilamellar spherical vesicles of DPPC. Left column: overlaid spectra for vesicles containing 25% (red) and 35% molar ratio (blue) of MT. Central column: overlaid spectra for vesicles of pure DPPC (black) and containing 25% molar ratio of MT (red). Right column: overlaid spectra for vesicles of pure DPPC (black) and containing 25% molar ratio of MT (red) recorded with a different spin probe. Numbers indicate the temperature (°C) of each sample. Total magnetic field scan range: 100 G. (For interpretation of the references to color in this figure legend, the reader is referred to the web version of the article.)

vesicles containing 50 μM of MT was fitted to a monoexponential function. In this way a probe rotational correlation time of 1.14 ns was obtained, comparable to the value of 1.27 ns measured in the absence of MT (Fig. 4). Moreover, both the initial and residual anisotropies were little affected by the presence of the drug in the bilayer. The fluorescent group of Ahba locates in the polar head-group region of the lipid bilayer and therefore these results indicate that the presence of MT does not change substantially the microenvironment of the probe in that region.

3.2. Effect of miltefosine on SC membranes

According to previous work (Alonso et al., 1995, 1996), the EPR spectra of SC membranes, spin-labeled as described above,

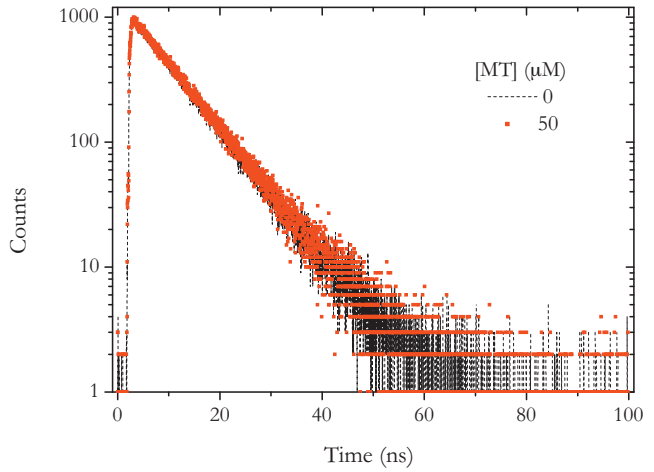

Fig. 3. The effect of miltefosine (MT) on the fluorescence decay of Abha in large unilamellar vesicles of DPPC. Picosecond-resolved intensity decay of Ahba fluorescence (20 μM) with (red dots) and without (black dots) 50 μM miltefosine. λ_{exc} = 330 nm, λ_{em} = 400 nm, T = 50 °C. (For interpretation of the references to color in this figure legend, the reader is referred to the web version of the article.)

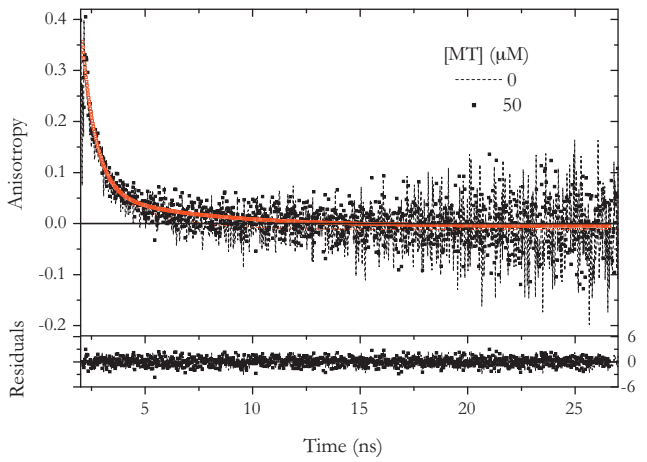

Fig. 4. The effect of miltefosine (MT) on the fluorescence anisotropy decay of Abha in large unilamellar vesicles of DPPC in the fluid phase. The experimental picosecond-resolved decay of Ahba fluorescence anisotropy (noisy black dots) and the corresponding fitted function (red) with and without 50 μM miltefosine are virtually identical. Probe concentration 20 μM, λ_{exc} = 330 nm, λ_{em} = 400 nm, T = 50 °C. (For interpretation of the references to color in this figure legend, the reader is referred to the web version of the article.)

indicate that these spin probes are distributed throughout the lipid domain of the tissue. The EPR spectra of probe 5-DSA incorporated to intercellular membranes of SC containing also MT are shown in Fig. 5A. Increasing the concentration of MT gradually reduces the EPR parameter $2A_{//}$, which we interpret as due to the increased fluidity of the probe microenvironment. $2A_{//}$ is a static parameter associated with the orientational distribution of the spin label in the membrane, which is widely used to monitor membrane fluidity. At 4% MT the decrease in $2A_{//}$ was of 10 G, which would correspond to a large increase of fluidity (Fig. 5B).

3.3. Temperature dependence of the MT interaction with SC lipids

Experimental and best-fit EPR spectra of several spin labels in SC membranes are shown in Fig. 6. At higher temperatures the spectra of 5-DSA was best fitted with a model of two components, corresponding to two populations of spin probe molecules with different mobility. The presence of the two components in the spectrum is clearly visible and these spectral features have already been discussed in previous works (de Queirós et al., 2005; dos Anjos et al., 2007a,b). The origin of these two spectral components is poorly understood and has been associated with hydrogen bond interactions between the polar head-group of the spin label and the polar interface of the membrane. The less mobile component 1 was assigned to the population of spin label molecules that are H-bonded to polar head-groups of the membrane lipids, while the more mobile component 2 was associated with spin label molecules in which this specific interaction has been replaced by H-bonding with water molecules. As indicated above, a two-component model was used to obtain an average correlation time τ_c. The fitting program provides the rotational correlation time τ_{ci} and fractional population population N_i for each individual component (i = 1, 2). Thus, the average rotational correlation time was calculated as $\tau_c = N_1 \times \tau_{c1} + N_2 \times \tau_{c2}$, It can be seen in Fig. 6 that the spectra of 5-DMS in SC at 30 °C is similar to that for SC treated with 4% MT at 10 °C, suggesting that the change in fluidity caused by MT is equivalent to that due to a temperature increase of about 20 °C for this sample.

The temperature dependence of EPR parameters of spin label 5-DSA in SC with and without 4% (w/w) MT is shown in Fig. 7. The changes in motion parameters, $2A_{//}$ and τ_c, are greater for

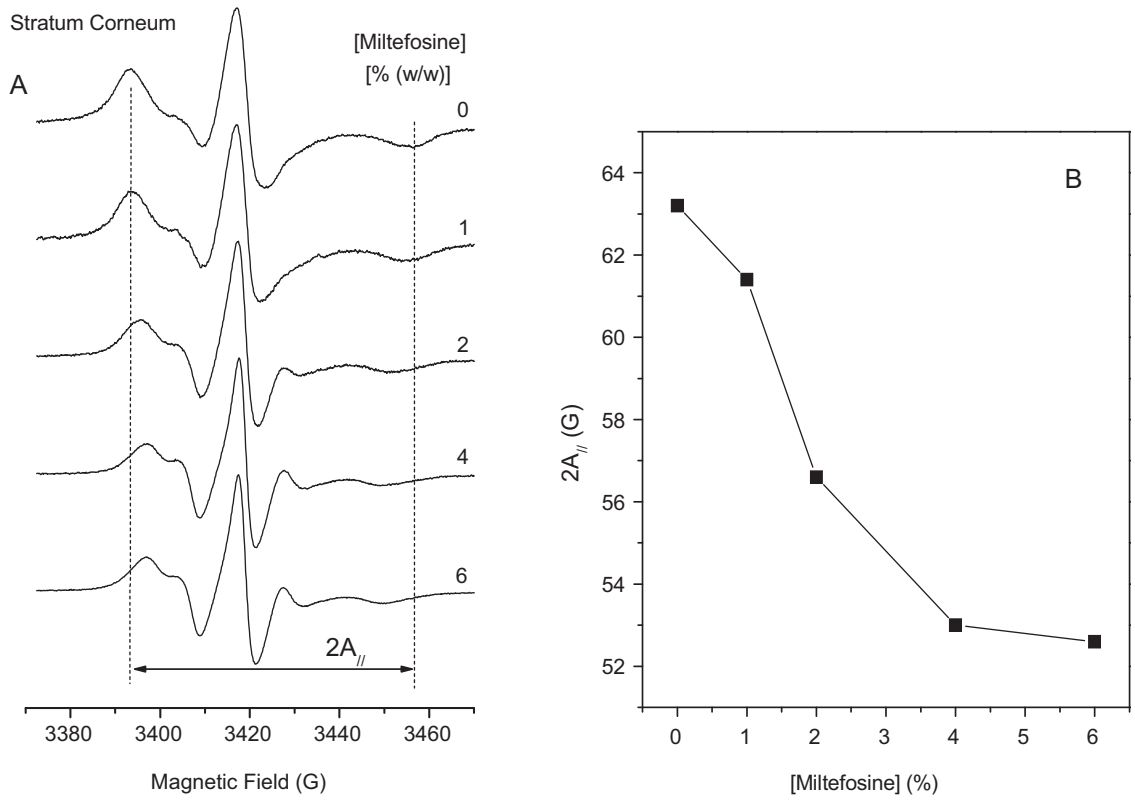

Fig. 5. (A) Effect of miltefosine (MT) on the EPR spectra of the probe 5-DSA in stratum corneum (SC); $T = 24\,^{\circ}C$. (B) Plot of the outer hyperfine splitting parameter $2A_{//}$ obtained from the EPR spectra as a function of MT concentration. Error bar: 0.5 G.

temperatures around 30 °C and tend to disappear at temperatures around 60–70 °C. The spectral simulation allows a more complete analysis taking into account the spectrum as a whole, and provides a parameter that best represents the motion of the nitroxide moiety. It is noteworthy that for the EPR spectra (42–70 °C) simulated with two components, the presence of MT gives rise to both an increase of the molecular dynamics of components 1 and 2 and also an augmented population of the faster component 2.

The polar head-group in spin labels 5- and 16-DMS is an H-bond acceptor carbonyl group while that of 5-DSA is a carboxylic group, with both donor and acceptor groups. As a result of that, it would be expected that 5- and 16-DMS probes would interact more weakly with the polar membrane interface, and probably because of this, they yield two-component spectra at much lower temperatures (Fig. 8). The more lipophilic spin labels 5- and 16-DMS would show a relatively larger fraction of the faster component 2, and the presence of MT seems to favor that trend. Since the nitroxide radical of spin label 16-DMS is located at the end of the acyl chain, the observed rotational diffusion is much faster than that of the 5-substituted probes. Nevertheless, the general thermal behavior was similar for the three spin probes used in this work. At 60 °C the effect of MT disappears and tends to reverse for higher temperatures.

To examine whether MT may change the dynamics of the major lipid components of SC, spherical vesicles were prepared with bovine brain ceramide, behenic acid and cholesterol in molar ratio (2:1:1) to represent the three major lipid classes of SC. The EPR spectra of 5-DSA in these vesicles with or without 20 mol% MT (not shown) indicated that MT caused a small decrease in the fluidity of the lipid bilayer, contrary to expectation.

4. Discussion

Miltefosine (MT) is a single-chain phospholipid with a phosphocholine polar head-group as in the DPPC molecule. Moreover, the simple C(16) alkyl chain of MT is of the same length as the double alkyl chain of DPPC. MT forms micelles at very low c.m.c., with values reported in the 2.0–35 μM range (Rakotomanga et al., 2004; Macdonald et al., 1991), consistent with the conical shape of the molecule. The phosphocholine headgroup is a zwitterion in an extense pH range (Rey Gómez-Serranillos et al., 2004; Kaznessis et al., 2002) therefore both DPPC and MT should be in zwitterionic form in the experimental conditions used in the present work. A study of the interaction of MT with monolayers of POPC or sterols has shown that MT molecules in the 10^{-6} M concentration range insert into the monolayer as monomers. At higher MT concentration, the micelles reaching the interface were deployed as groups of monomers into the POPC or sterol monolayer (Rakotomanga et al., 2004). In the present work, the interaction of MT with large unilamelar spherical vesicles of DPPC has been studied with both spin and fluorescent probes. The experimental parameters recorded in fluorescence experiments are, of course, very different from those of the EPR experiments. However, sampling time and length scale is very similar, providing the physical basis for the correlation of the experimental information obtained from the two techniques (van Ginkel et al., 1986).

The expected ~100 nm diameter of the vesicles is at least 10 times smaller than that of a typical cell and thus, the smaller curvature should favor micelle formation. The EPR spectra of the spin labels used in this work, when incorporated to micelles of MT (data not shown) indicated a much higher mobility of the probes than in DPPC spherical bilayers. Therefore, any fraction of micelles that could be present in the DPPC-MT vesicles would be easily detected from its characteristic spectral component. However, the EPR signal of MT micelles was not detected in DPPC vesicles as well as in those prepared with ceramide, fatty acid and cholesterol. On the contrary, homogeneous EPR signals were observed, indicating that MT molecules were essentially as monomers well distributed in these vesicles. The apparent pK_a of the 5-DSA spin label is 7.2, as

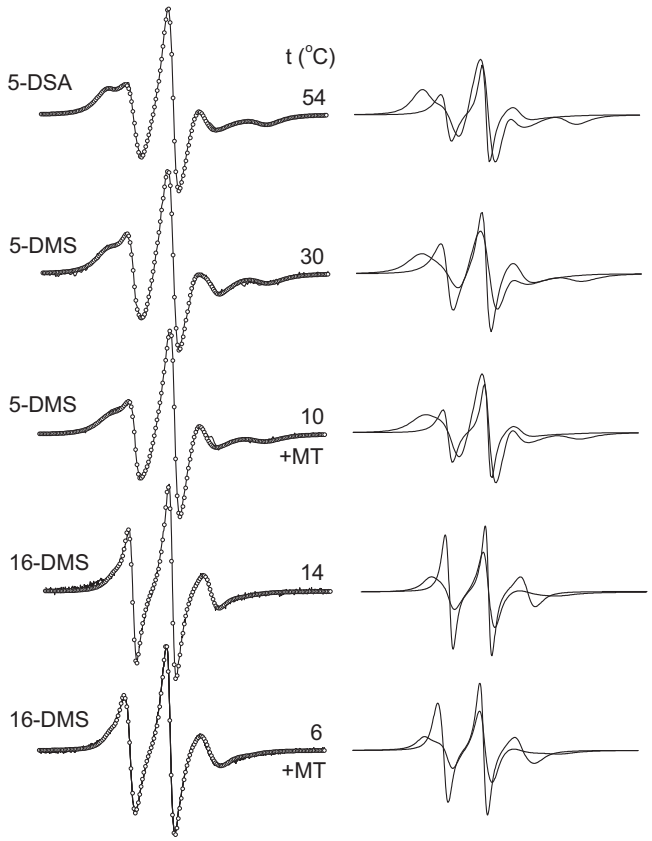

Fig. 6. Left column: experimental EPR spectra (continuous line) and best-fit (empty circles) of several spin labels in stratum corneum membranes (SC) at the indicated temperatures. The spectra labeled with +MT corresponds to SC samples treated with 4% MT (w/w). Right column: analysis of the spectra using a two-component model. EPR spectra of 5-DSA and 5-DMS probes were simulated with the fitting program NLLS and those of 16-DMS with the EPRSIM program, using a model of two spectral components.

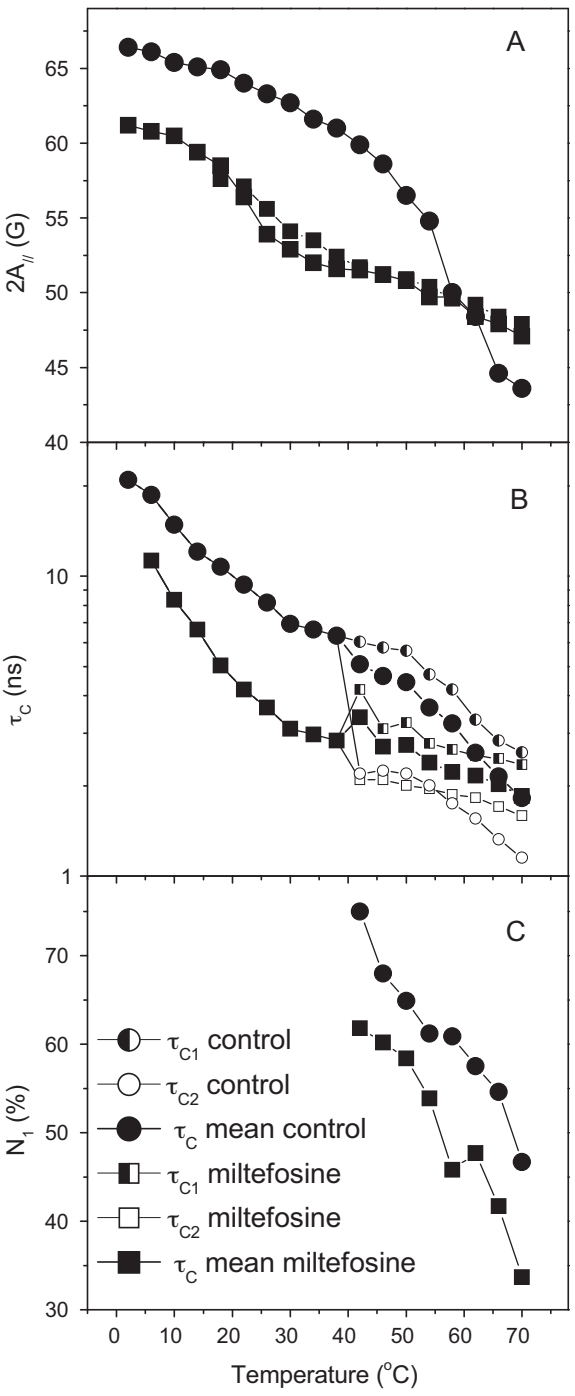

Fig. 7. EPR parameters of spin label 5-DSA in stratum corneum (squares) and in the same samples treated with 4% (w/w) miltefosine (circles) as a function of temperature. Panel A: parameter $2A_{//}$, measured directly from the EPR spectra (Fig. 2); Panel B: rotational correlation time, τ_c/ns (log scale); Panel C: fractional population of component 1. These last parameters are best-fit values obtained with the NLLS program using models of one or two spectral components. The average τ_c was calculated from $\tau_c = N_1 \times \tau_{c1} + N_2 \times \tau_{c2}$.

estimated in DPPC bilayers (Perez-Gil et al., 1995), whereas the 5- and 16-DMS probes are not ionizable. The EPR measurements of the spin-labels presented here probed different parts of the transversal lipid bilayer structure. These measurements show that the presence of relatively large amounts of the drug did not change noticeably the bilayer structure being probed.

Fluorescence depolarization experiments extended further the range on the lipid bilayer being probed, because the emitting group of the Ahba probe locates preferentially at the polar interface of the DPPC bilayer. The fluorescence spectral properties of the probe Ahba in DPPC spherical vesicles containing MT were virtually the same as in water solution, indicating that this part of the bilayer is not affected by the presence of the drug.

In the case of SC, the samples were first labeled with the spin probe and then treated with MT. It was observed that the EPR spectrum of these samples was due to the spin probe embedded within the SC intercellular membranes, without any signal due to MT micelles. The EPR measurements were performed at pH 5.5, to reproduce native conditions (Öhman and Vahlquist, 1998), and in the presence of EDTA, to prevent reduction of the spin probes by residual amounts of metallic ions. Control measurements in the absence of EDTA or suspending SC membranes in PBS buffer, pH 7.4 showed that the MT effect reported above was not abolished. In addition, SC samples measured immediately after their preparation (without dehydration) presented also the same effect.

As shown above, miltefosine gives rise to a large increase in the fluidity of intercellular membranes of SC, while on the other hand does not produce the similar effect in model membranes prepared with the SC major lipid components. This is interpreted as due to the structural differences between the lamellar structure of SC and the bilayer of the membrane models. In fact, the SC lipid chain dynamics is very different from that of vesicles prepared with SC lipids extracted with mixtures of organic solvents (Alonso et al., 2000). Thus, the value of the $2A_{//}$ parameter (Fig. 2), measured at room temperature for the probe 5-DSA in spherical vesicles made up from lipids extracted from SC and directly in SC intercellular membranes

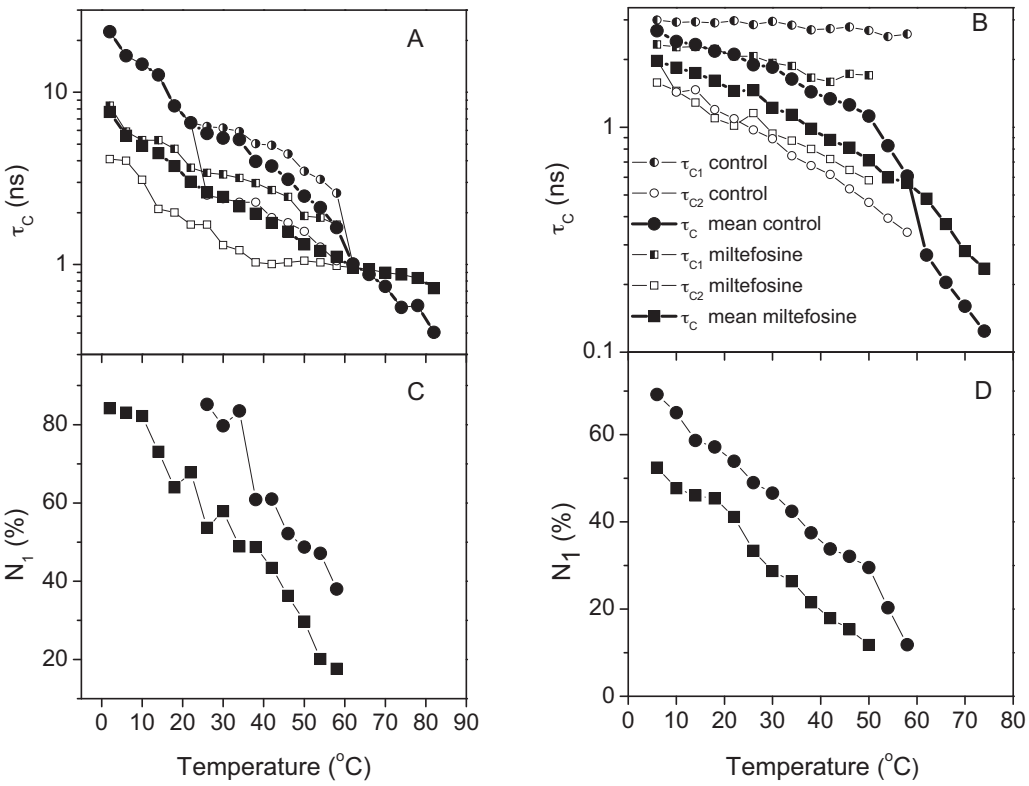

Fig. 8. EPR rotational correlation time, τ_c, and fractional population of component 1, N_1, of spin label 5-DMS (A, C) and 16-DMS (B and D) in stratum corneum (circles) and in the same samples treated with 4% (w/w) MT (squares) as a function of temperature. These parameters are best-fit values obtained with the NLLS program using models of one or two spectral components. The average τ_c was calculated as: $\tau_c = N_1 \times \tau_{c1} + N_2 \times \tau_{c2}$.

are 56 and 63 G, respectively. Interesting, the $2A_{//}$ room temperature vesicle value is similar to that of SC membranes at 50 °C (Alonso et al., 2000). The current model of the intercellular lipid lamellae structure of SC is mainly based on electron density profiles from transmission electron micrographs of SC membranes (Hill and Wertz, 2003) and in the 13 nm lamellar periodicity measured by small angle X-ray diffraction (Bouwstra et al., 1991). The three-band pattern observed between the edges of adjacent corneocytes corresponds to two monolayers of covalently bound hydroxyceramides, on the outer surfaces of the cornified envelopes, and to a central lamella which is a simple bilayer without interdigitation of the acyl chains (Hill and Wertz, 2003). The SC membrane rigidity is very likely due to the protein layer bound to the hidroxyceramide lipid envelope. The restricted lipid mobility results from the lipid fraction bound to proteins on one side of the monolayer and on the other side because of the low-mobility interface characteristic of the lipid polar groups.

5. Conclusions

The interaction of the anticancer and antileishmanial drug miltefosine (MT) with large unilamellar vesicles of DPPC and membranes from stratum corneum (SC) was studied here by spin probes and steady-state and time-resolved fluorescence probe methods. No significant changes were observed in the DPPC model lipid bilayers in the presence of 25–35% molar ratio of the drug. Similarly, a very modest effect of MT was recorded in model spherical bilayers made up from lipids extracted from SC. In contrast, MT gives rise to a large increase in the fluidity of intercellular membranes of stratum corneum (SC), both at the polar head-group interface and at the internal lipophilic region of the membranes. The drug effect decreases at higher temperatures, disappearing near 60 °C, when the membranes are much more fluid, suggesting that MT may behave as an acyl-chain spacer. In that case, when the membrane is very fluid MT molecules are easily incorporated with little perturbation of the underlying structure. These results indicate that the complex protein–lipid architecture of the corneocyte envelope, which is lost in model membranes prepared from extracted lipids, is responsible for the observed changes in lipid fluidity. This information may be relevant for the development of a topical treatment of cutaneous leishmaniasis with MT or in combination with other drugs.

Acknowledgments

This work was supported by Brazilian research funding agencies CNPq, CAPES, FUNAPE, FAPESP and MCINN-Spain, Grant CTQ2010/16457 (AUA). L. Alonso, S.A. Mendanha and M. Berardi are recipients of fellowships from CNPq, CAPES and FAPESP, respectively. A. Alonso and A.S. Ito gratefully acknowledge the CNPq for their research grants, A.S. Ito is a member of INCT FCx.

References

Alonso, A., Meirelles, N.C., Tabak, M., 1995. Effect of hydration upon the fluidity of intercellular membranes of stratum corneum: an EPR study. Biochim. Biophys. Acta 1237, 6–15.

Alonso, A., Meirelles, N.C., Yushmanov, V.E., Tabak, M., 1996. Water increases the fluidity of intercellular membranes of stratum corneum: correlation with water permeability, elastic, and electrical properties. J. Invest. Dermatol. 106, 1058–1063.

Alonso, A., Meirelles, N.C., Tabak, M., 2000. Lipid chain dynamics in stratum corneum studied by spin label electron paramagnetic resonance. Chem. Phys. Lipids 104, 101–111.

Alonso, A., dos Santos, W.P., Leonor, S.J., Tabak, M., 2001. Stratum corneum protein dynamics as evaluated by a spin-label maleimide derivative: effect of urea. Biophys. J. 81, 3566–3576.

Alonso, A., da Silva, J.V., Tabak, M., 2003. Hydration effects on the protein dynamics in stratum corneum as evaluated by EPR spectroscopy. Biochim. Biophys. Acta 1646, 32–41.

Alvar, J., Croft, S., Olliaro, P., 2006. Chemotherapy in the treatment and control of leishmaniasis. Adv. Parasitol. 61, 223–274.
Arsov, Z., Schara, M., Strancar, J., 2002. Quantifying the lateral lipid domain properties in erythrocyte ghost membranes using EPR-spectra decomposition. J. Magn. Reson. 157, 52–60.
Barrat, G., Saint-Pierre-Chazalet, M., Loiseau, PhM., 2009. Cellular transport and lipid interactions of miltefosine. Curr. Drug Metabol. 10, 247–255.
Berman, J.D., 2006. Development of miltefosine for the leishmaniasis. Mini Rev. Med. Chem. 6, 145–151.
Bouwstra, J.A., Gooris, G.S., van der Spek, J.A., Bras, W., 1991. Structural investigations of human stratum corneum by small angle X-ray scattering. J. Invest. Dermatol. 97, 1005–1012.
Budil, D.E., Lee, S., Saxena, S., Freed, J.H., 1996. Nonlinear-least-squares analysis of slow-motional EPR spectra in one and two dimensions using a modified Levenberg–Marquardt algorithm. J. Magn. Reson. A 120, 155–189.
Camargos, H.S., Silva, A.H.M., Anjos, J.L.V., Alonso, A., 2010. Molecular dynamics and partitioning of di-tert-butyl nitroxide in stratum corneum membranes: effect of terpenes. Lipids 45, 419–427.
Croft, S.L., Seifert, K., Duchene, M., 2003. Antiprotozoal activities of phospholipid analogues. Mol. Biochem. Parasitol. 126, 165–172.
Croft, S.L., Barrett, M.P., Urbina, J.A., 2005. Chemotherapy of trypanosomiases and leishmaniasis. Trends Parasitol. 21, 508–512.
Croft, S.L., Sundar, S., Fairlamb, A.H., 2006. Drug resistance in leishmaniasis. Clin. Microbiol. Rev. 19, 111–126.
de Queirós, W.P., Neto, D.D., Alonso, A., 2005. Dynamics and partitioning of spin-labeled stearates into the lipid domain of stratum corneum. J. Control. Release 106, 374–385.
dos Anjos, J.L.V., Alonso, A., 2008. Terpenes increase the partitioning and molecular dynamics of an amphipathic spin label in stratum corneum membranes. Int. J. Pharm. 350, 103–112.
dos Anjos, J.L.V., Neto, D.D., Alonso, A., 2007a. Effects of ethanol/L-menthol on the dynamics and partitioning of spin-labeled lipids in the stratum corneum. Eur. J. Pharm. Biopharm. 67, 406–412.
dos Anjos, J.L.V., Neto, D.D., Alonso, A., 2007b. Effects of 1,8-cineole on the dynamics of lipids and proteins of stratum corneum. Int. J. Pharm. 345, 81–87.
Hill, J.R., Wertz, P.W., 2003. Molecular models of the intercellular lipid lamellae from epidermal stratum corneum. Biochim. Biophys. Acta 1616, 121–126.
Hohl, D., 1990. Cornified cell envelope. Dermatologica 180, 201–221.
Jha, T.K., Sundar, S., Thakur, C.P., Bachmann, P., Karbwang, J., Fischer, C., Voss, A., Berman, J., 1999. Miltefosine, an oral agent, for the treatment of Indian visceral leishmaniasis. N. Engl. J. Med. 341, 1795–1800.
Kaznessis, Y.N., Kim, S., Larson, R.G., 2002. Simulations of zwitterionic and anionic phospholipid monolayers. Biophys. J. 82, 1731–1742.
Kuhlencord, A., Maniera, T., Eibl, H., Unger, C., 1992. Hexadecylphosphocholine: oral treatment of visceral leishmaniasis in mice. Antimicrob. Agents Chemother. 36, 1630–1634.
Macdonald, P.M., Rydall, J.R., Kuebler, S.C., Winnik, F.M., 1991. Synthesis and characterization of a homologous series of zwitterionic surfactants based on phosphocholinet. Langmuir 7, 2602–2606.
Marquezin, C.A., Hirata, I.Y., Juliano, L., Ito, A.S., 2006. Spectroscopic characterization of 2-amino-N-hexadecyl-benzamide (AHBA), a new fluorescence probe for membranes. Biophys. Chem. 124, 125–133.
Masukawa, Y., Narita, H., Shimizu, E., Kondo, N., Sugai, Y., Oba, T., Homma, R., Ishikawa, J., Takagi, Y., Kitahara, T., Takema, Y., Kita, K., 2008. Characterization of overall ceramide species in human stratum corneum. J. Lipid Res. 49, 1466–1476.
Öhman, H., Vahlquist, A., 1998. The pH Gradient over the stratum corneum differs in x-linked recessive and autosomal dominant ichthyosis: a clue to the molecular origin of the acid skin mantle? J. Invest. Dermatol. 111, 674–677.
Perez-Gil, J., Casals, C., Marsh, D., 1995. Interactions of hydrophobic lung surfactant proteins SP-B and SP-C with dipalmitoylphosphatidylcholine and dipalmitoylphosphatidylglycerol bilayers studied by electron spin resonance spectroscopy. Biochemistry 34, 3964–3971.
Rakotomanga, M., Loiseau, P.M., Saint-Pierre-Chazalet, M., 2004. Hexadecylphosphocholine interaction with lipid monolayers. Biochim. Biophys. Acta 1661, 212–218.
Rey Gómez-Serranillos, I., Miñones Jr., J., Dynarowycz-Latka, P., Iribarnegaray, E., Casas, M., 2004. Study of the Π–*A* isotherms of miltefosine monolayers spread at the air/water interface. Phys. Chem. Chem. Phys. 6, 1580–1586.
Saugar, J.M., Delgado, J., Hornillos, V., Luque-Ortega, J.R., Amat-Guerri, F., Acuña, A.U., Rivas, L., 2007. Synthesis and biological evaluation of fluorescent leishmanicidal analogues of hexadecylphosphocholine (Miltefosine) as probes of antiparasite mechanism. J. Med. Chem. 50, 5994–6003.
Sindermann, H., Engel, J., 2006. Development of miltefosine as an oral treatment for leishmaniasis. Trans. R. Soc. Trop. Med. Hyg. 100 (Suppl. 1), S17–S20.
Soto, J., Soto, P., 2006. Miltefosine: oral treatment of leishmaniasis. Expert Rev. Anti Infect. Ther. 4, 177–185.
Stopar, D., Strancar, J., Spruijt, R.B., Hemminga, M.A., 2006. Motional restrictions of membrane proteins: a site-directed spin labeling study. Biophys. J. 91, 3341–3348.
Swartzendruber, D.C., Wertz, P.W., Madison, K.C., Downing, D.T., 1987. Evidence that the corneocyte has a chemically bound lipid envelope. J. Invest. Dermatol. 88, 709–713.
van Ginkel, G., Korstanje, L.J., van Langen, H., Levine, Y.K., 1986. Correlation between orientational order and reorientational dynamics of probe molecules in lipid bilayers. Faraday Discuss. Chem. Soc. 81, 49–61.
Wertz, P.W., Downing, D.T., 1987. Covalently bound ω-hydroxyacylsphingosine in the stratum corneum. Biochim. Biophys. Acta 917, 108–111.
Wertz, P.W., Madison, K.C., Downing, D.T., 1989. Covalently bound lipids of human stratum corneum. J. Invest. Dermatol. 92, 109–111.
Wieder, T., Reutter, W., Orfanos, C.E., Geilen, C.C., 1999. Mechanisms of action of phospholipid analogs as anticancer compounds. Prog. Lipid Res. 38, 249–259.